

# A New Method for the Calculation of the Hot-Spot Temperature in Power Transformers With ONAN Cooling

Zoran Radakovic and Kurt Feser, *Fellow, IEEE*

**Abstract**—In the previous work of the authors, an original thermal model of transformers with ONAN cooling was developed. The model takes into account the influence of nonlinear thermal characteristics in transient thermal processes; instead of exponential functions and time constants, the numerical solution of differential equations is used. The model delivers one characteristic temperature in copper (solid insulation) and one characteristic temperature in oil. In this paper, the analysis stresses the definition of the hot-spot temperature of the solid insulation by using easily measurable quantities. Then, the parameters of the model can be precisely determined from inexpensive measurements in a short-circuit heating experiment and the model can deliver the hot-spot temperature. The experimental base of this research are the measurements on a 630-kVA,  $3 \times 10$  kV/ $3 \times 6$  kV ONAN transformer equipped with 112 temperature sensors (102 inside the central positioned 10-kV winding).

**Index Terms**—Hot-spot temperature, power transformer thermal factors, thermal modeling.

## I. INTRODUCTION

THE hot spot insulation temperature represents the most important limiting factor of a transformer loading. The hot-spot temperature has to be under a prescribed limit value. A cumulative effect of insulation aging, depending on time change of hot-spot temperature, should be less than a planned value. That is why there exists an interest to know the hot-spot temperature in every moment of a real transformer operation in the conditions of variable load and ambient air temperature. Possible approaches are to measure the hot-spot temperature (using fiber-optics technique) or to calculate it, using a thermal model of power transformer. Due to the complexity of the phenomena, there exists no exact thermal model. A thermal model can be created to deliver [1]: a) the temperature distribution over the whole winding, or b) the temperature values at the characteristic points.

The originally developed algorithm (thermal model) for temperature calculation [2] is based on characteristic temperatures. The algorithm is established on the following two fundamentals: 1. To describe as much as possible the real physic of heat transfer; first of all the influence of nonlinear heat transfer characteristics to the transient thermal behavior and 2. To deter-

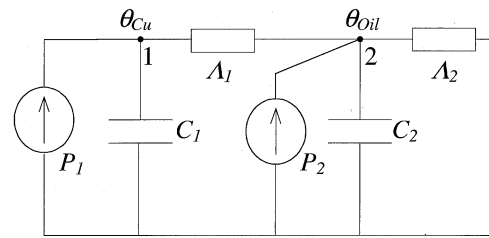


Fig. 1. Thermal network with two nodes.

mine the thermal model parameters for a specific transformer type without complicated and expensive tasks (in contrast to the models from [3] and [4]).

The algorithm is till now proofed on different transformers loaded in short circuit heating tests and in normal operation, but was never verified by direct hot-spot temperature measurement. This verification is done and is presented in this paper. A new way of the characteristic temperature definition, compared to the previously used one [2], is proposed in order to reduce the error in the hot-spot temperature calculation. Besides the natural need to check the precision of the hot-spot temperature calculation, this work is also inspired by the new draft of relevant IEC standard [5].

## II. SHORT DESCRIPTION OF THE ORIGINAL THERMAL MODEL

The thermal model is based on thermal network shown in Fig. 1.

$P_1$	power loss in windings;
$P_2$	power loss in core and tank;
$A_1$	heat conductance of the heat transfer from windings to oil;
$A_2$	heat conductance of the heat transfer from oil to air;
$C_1$	winding heat capacity;
$C_2$	heat capacity of oil, core, and tank;
$\theta_{Cu}$	copper characteristic temperature rise;
$\theta_{Oil}$	oil characteristic temperature rise.

Temperature increases (rises) are calculated with respect to the temperature of the air surrounding the transformer.

The system is nonlinear due to the temperature dependent thermal conductances. The most convenient and commonly used [6] dependencies are

$$\Lambda_1 = K_1(\theta_{Cu} - \theta_{Oil})^{n_1} \quad (1)$$

$$\Lambda_2 = K_2(\theta_{Oil})^{n_2}. \quad (2)$$

Manuscript received September 2, 2002. This work was supported in part by Alexander von Humboldt Foundation.

The authors are with the Institute of Power Transmission and High Voltage Technology, University of Stuttgart, Stuttgart 70569, Germany (e-mail: radakovic@etf.bg.ac.yu; feser@ieh.uni-stuttgart.de).

Digital Object Identifier 10.1109/TPWRD.2003.817740

The parameters  $K_1$ ,  $n_1$ ,  $K_2$ ,  $n_2$ ,  $C_1$ , and  $C_2$  are determined by the developed procedure [2] from the values of measured characteristic temperatures in a short-circuit heating experiment. The characteristic temperatures can be adopted liberally, but preferably by using easily measurable temperatures: local values outside the tank and average winding temperature; the method for continuous average temperature measurement is exposed in [7].

Temperature rises  $\theta_{Cu}$  and  $\theta_{Oil}$  in discrete time moments (period  $\Delta t$ ) can be calculated from the equations

$$\begin{aligned}\theta_{Cu,k+1} &= \theta_{Cu,k} + \frac{\Delta t}{C_1} (P_1 - \Lambda_{1,k}(\theta_{Cu,k} - \theta_{Oil,k})) \\ &= \theta_{Cu,k} + \frac{\Delta t}{C_1} (P_1 - K_1(\theta_{Cu,k} - \theta_{Oil,k})^{n_1+1}) \\ \theta_{Oil,k+1} &= \theta_{Oil,k} + \frac{\Delta t}{C_2} (P_2 + \Lambda_{1,k}(\theta_{Cu,k} - \theta_{Oil,k}) \\ &\quad - \Lambda_{2,k}\theta_{Oil,k}) \\ &= \theta_{Oil,k} + \frac{\Delta t}{C_2} (P_2 + K_1(\theta_{Cu,k} - \theta_{Oil,k})^{n_1+1} \\ &\quad - K_2\theta_{Oil,k}^{n_2+1}).\end{aligned}\quad (4)$$

The power loss distribution in a short-circuit heating experiment and during normal operation is considered in [1].

### III. SELECTION OF COPPER AND OIL CHARACTERISTIC TEMPERATURES

It is natural to choose the most critical temperatures: solid insulation hot-spot and top oil. In a previous work of the authors [1], [2], these values were used, where the hot-spot temperature ( $\vartheta_{hs}$ ) was calculated based on the following measured temperatures: mean winding temperature ( $\vartheta_{Cua}$ ), top-oil temperature ( $\vartheta_{to}$ ), and temperatures of the radiator outer surface—at the top ( $\vartheta_{rt}$ ) and the bottom ( $\vartheta_{rb}$ ). The formula, expressed by temperature rise values, to calculate the hot-spot is

$$\theta_{hs}^* = \theta_{to} + H \left( \theta_{Cua} - \left( \theta_{to} - \frac{\theta_{rt} - \theta_{rb}}{2} \right) \right). \quad (5)$$

$H$  represents the hot-spot factor, adopted to be equal 1.1.

Instead of using top-oil temperature, the bottom oil could be used. Then, the previous formulae turn into

$$\theta_{hs}^* = \theta_{bo} + \theta_{rt} - \theta_{rb} + H \left( \theta_{Cua} - \left( \theta_{bo} + \frac{\theta_{rt} - \theta_{rb}}{2} \right) \right). \quad (6)$$

From the easily measured temperatures in short-circuit heating experiment, the time change of  $\theta_{hs}^*$  can be defined and afterwards the thermal circuit parameters can be calculated. Using such defined thermal model and data of load and ambient air in real operation, the values of  $\vartheta_{hs}^*$  and  $\vartheta_{to}$  can be calculated in every moment. It is shown [2] that the procedure delivers high accurate results for temperatures  $\vartheta_{hs}^*$  and  $\vartheta_{to}$ . It is of essential importance to check the precision of expression (5), comparing the  $\vartheta_{hs}^*$  value with the real hot-spot temperature ( $\vartheta_{hs}$ ). For that purpose, direct measurements of the hot-spot temperature are needed. Two factors could disturb the precision of the expression (5). The first one is the hot-spot factor ( $H$ ), taking into account nonuniform power losses in windings, change of local

heat transfer coefficient over the winding height, and edge effects of oil streaming at winding ends. The precise definition of the hot-spot factor requires complicated calculations of the temperature distribution over the whole winding or/and demanding expensive measurements. A constant approximate value could be applied (as recommended in [5] and [6]) if it does not cause a high calculation error. This factor influences the steady state hot-spot temperature value. The second factor is the different dynamic characteristic of measured top temperatures (oil in the pocket and at the top of the radiators) from that determining the winding-oil heat exchange (oil at the top of the winding).

In addition, it is known [5] that the hot-spot minus oil in the pocket temperature difference has an overshoot when the load increases rapidly. Overshoot means that the temperature difference in transient process reaches a higher value than the value in steady-state with the same load level. High overshoot values could be expected: for ONAN transformers between 1.4 and 2 [5]. Although functional dependence (1) shows that the heat transfer from copper to oil increases quicker than copper temperature ( $P = \Lambda_1(\theta_{Cu} - \theta_{Oil})$ ;  $n_1 \geq 0$ ), it cannot model the temperature difference overshoot. The functional dependence of thermal conductance  $\Lambda_1$  cannot be easily defined to result with such a high overshoot. Consequently, an attempt with some other characteristic oil temperature, instead the top oil in the pocket temperature should be made.

### IV. EXPERIMENTAL RESEARCH

The positions of sensors built inside the central positioned 10-kV winding are shown in Fig. 2. Additional ten measuring points are: the oil entering (top) and exiting (bottom) the radiator, the top oil (two positions—in the pocket and in the central horizontal position), five positions at different height of the radiators outer surface, ambient temperature. The principal electrical schema of the experiment is given in [7]. During the transient thermal processes, the following 15 local temperatures were measured: 11 positions denoted in Fig. 2 [three positions at which the hot-spot could be expected—sensors S1-S3, oil in the cooling channel between the inner and the outer winding parts—sensors S4 and S5, oil near (3 mm) the outer surface of the winding—sensors S6 and S7, oil at 10 mm from the other winding surface—undisturbed oil mass—sensor S8, two positions at the winding top—sensors S9 and S10, one position at the winding bottom—sensor S11], the top and the bottom of the radiator, the top pocket oil, and the ambient. The values of the other temperatures were measured only in thermal steady-states at different constant transformer loads.

The series of heating experiments was done with different load profiles [2]. Steady states were reached at nine different loads, ranging from 27.4% to 124.2% of power loss due to rated current— $P_{Cu r} = 8790$  W; rated iron (no-load) power loss amounts to  $P_{Fe r} = 1875$  W.

### V. COPPER MINUS OIL TEMPERATURE DIFFERENCE

#### A. Steady-State Values

The value of the hot-spot factor is analyzed in this section. Table I contains characteristic temperatures registered under steady-state conditions at different transformer loads.  $\vartheta_{hsm1}$

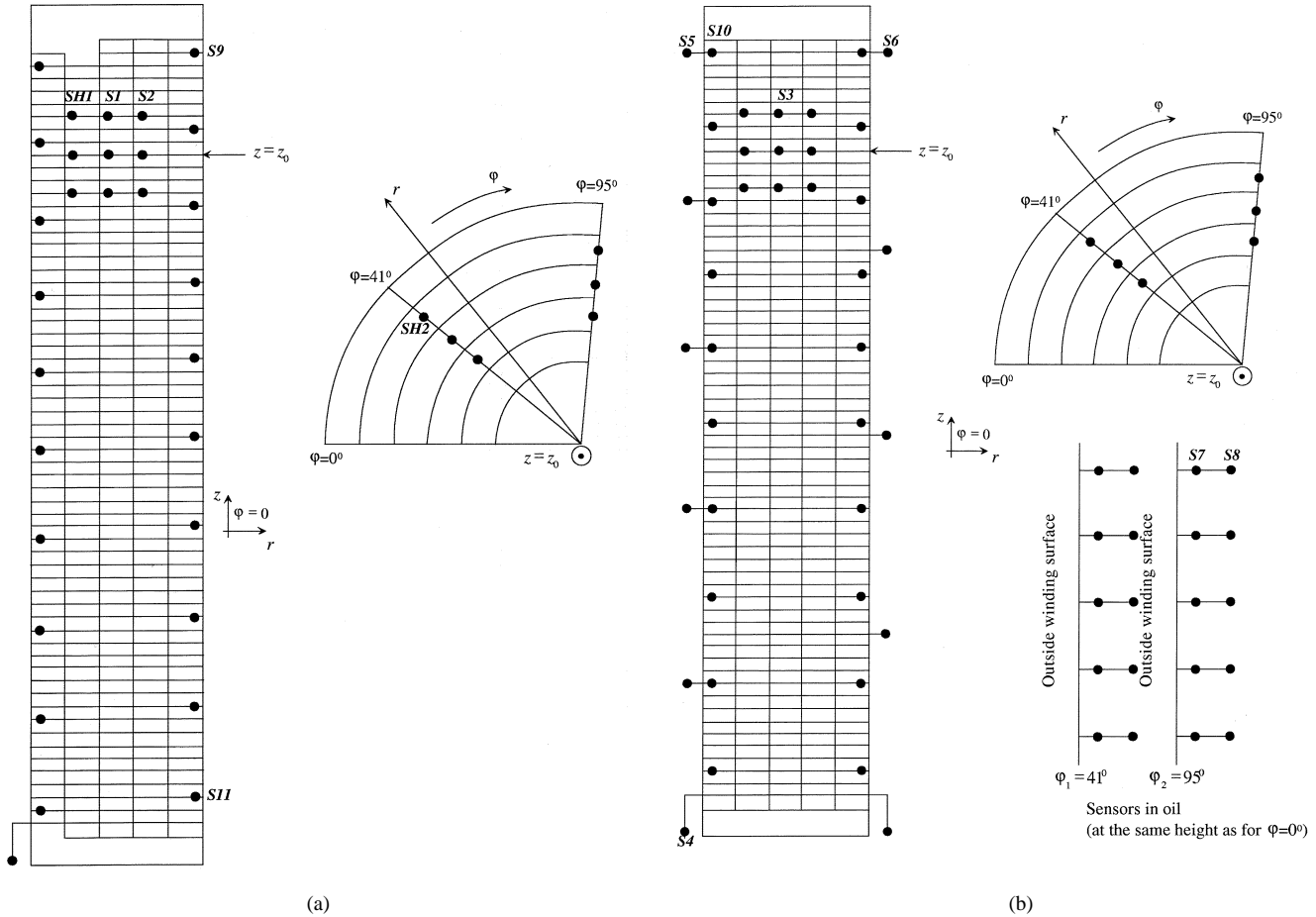


Fig. 2. Positions of temperature measuring sensors.

TABLE I  
CHARACTERISTIC TEMPERATURES UNDER STEADY-STATE CONDITIONS

Current at 6 kV side (A)	Power loss (W)	Temperature ( $^{\circ}\text{C}$ )									
		Ambient $\vartheta_a$	Hot- spot $\vartheta_{hsm1}$	Hot- spot $\vartheta_{hsm2}$	Average winding $\vartheta_{Cua}$	Top pocket oil $\vartheta_{top}$	Radiator top $\vartheta_{rt}$	Radiator bottom $\vartheta_{rb}$	Bottom oil $\vartheta_{bo}$	$\vartheta_{hsc} -$ $\vartheta_{hsm2}$	H
32	2347	16.8	45.8	47.7	38.4	37.6	38.2	23.3	24.7	-1.44	1.02
34.27	2671	19.5	50.5	51.5	41.0	41.4	42.2	25.5	27.2	-1.60	1.21
41.18	3769	13.2	54.2	56.4	43.6	42.0	43.5	22.4	24.9	-1.54	1.02
43.7	4441	16.6	64.7	67.4	53.8	50.7	53.0	29.8	34.2	-0.54	0.849
46.61	4992	18.4	69.1	70.4	56.0	55.6	58.9	34.6	34.9	-1.46	1.12
52.54	6333	11.1	70.3	72.6	54.6	53.0	55.8	26.5	30.6	-2.08	1.08
60.00	8667	14.0	91.1	94.6	73.8	69.6	74.1	38.3	44.2	-1.73	0.949
63.79	9686	5.02	89.3	90.1	71.4	67.1	71.9	33.9	38.1	1.62	0.930
65.6	10636	10.4	100.4	103.8	82.8	73.9	80.3	40.3	46.8	0.38	0.861

is the temperature measured by the sensor S1, appearing as the hottest measured copper temperature of those recorded during transient thermal processes and  $\vartheta_{hsm2}$  is the maximum registered copper temperature (by the sensors SH1 or SH2). Column  $\vartheta_{hsc} - \vartheta_{hsm2}$  contains the differences of hot-spot temperature calculated by the expression

$$\vartheta_{hsc} = \vartheta_{bo} + \vartheta_{rt} - \vartheta_{rb} + 1.1 \left( \vartheta_{Cua} - \left( \vartheta_{bo} + \frac{\vartheta_{rt} - \vartheta_{rb}}{2} \right) \right) \quad (7)$$

and measured hot-spot temperature  $\vartheta_{hsm2}$ . This error expresses the influence of approximate adopted value of factor  $H$  ( $H =$

1.1). Since the error is in the range  $(-2.08, +1.62)$  K the selection of the constant factor  $H$  is acceptable. In the last column, the values of factor  $H$ , calculated by

$$H = \frac{\vartheta_{hsm1} - (\vartheta_{bo} + \vartheta_{rt} - \vartheta_{rb})}{\vartheta_{Cua} - \left( \vartheta_{bo} + \frac{\vartheta_{rt} - \vartheta_{rb}}{2} \right)} \quad (8)$$

are exposed. Using these values of  $H$ , formula (6) delivers the exact steady-state temperature of the hot-spot measured by sensor S1 ( $\vartheta_{hsm1}$ ); in such a way it is possible to separate the influence of the specific dynamic of a radiator top temperature to the hot-spot temperature, discussed in the next section.

## B. Transients

1) *Hot-Spot Minus Top-Oil Temperature Difference:* In Fig. 3, the difference hot-spot temperature measured by the sensor S1 minus top pocket oil temperature is shown. The record is valid for the short-circuit heating experiment with constant loss equal to the power loss due to rated current (8790 W), starting at transformer temperature equal to ambient temperature.

There exists the temperature difference ( $\Delta\theta$ ) overshoot. The further investigation of  $\Delta\theta$  is done in different tests. For the comparison, normalized temperature difference values are used  $\Delta\theta_{rel} = (\Delta\theta - \Delta\theta_i) / (\Delta\theta_s - \Delta\theta_i)$ , where  $\Delta\theta_i$  is the starting value and  $\Delta\theta_s$  is the steady-state value corresponding to a new load. In the procedure from [5], it is supposed that the time

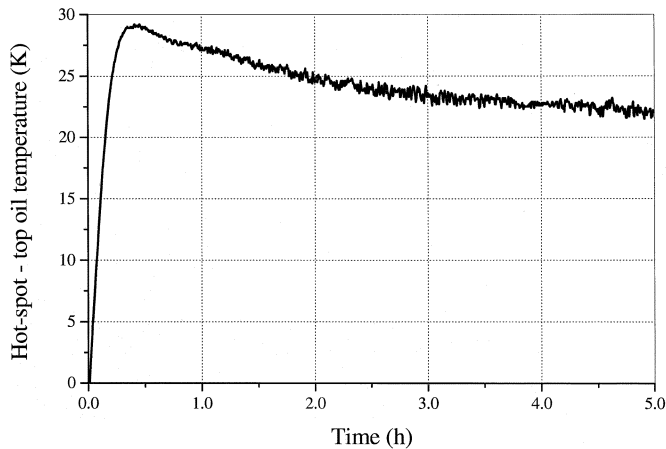


Fig. 3. Hot-spot minus top pocket oil temperature.

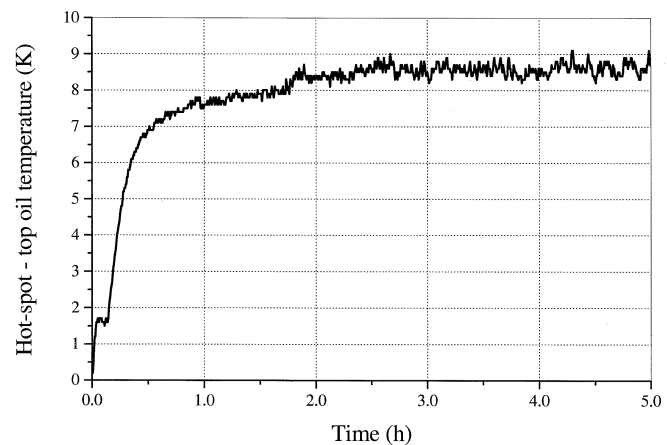


Fig. 4. Hot-spot minus top channel oil temperature.

TABLE II  
DATA OF THE HOT-SPOT TO TOP POCKET OIL TEMPERATURE DIFFERENCE

Power from / to	Max $\Delta\theta_{rel}$ reached at	$\Delta\theta_i$ (K)	$\Delta\theta_s$ (K)	Max $\Delta\theta_{rel}$
0 / 3769 W	0.55 h	0	12.2	1.39
0 / 6333 W	0.48 h	0	17.3	1.48
0 / 8667 W	0.45 h	0	21.5	1.35
6333 / 9686 W	0.58 h	17.3	22.2	1.12
4441 / 10636 W	0.5 h	14	26.5	1.15

change of  $\Delta\theta_{rel}$  is always the same, meaning also the maximum  $\Delta\theta_{rel}$  value is constant. Some results of the tests are shown in Table II.

The overshoot value ( $\max \Delta\theta_{rel}$ ) changes with the change of the load. At least two different values have to be introduced—the first one when a transformer is loaded from cold conditions (temperatures equal to the ambient temperature) and the second one when the load changes from lower value to higher value or opposite. If the value of  $\max \Delta\theta_{rel} = 1.4$  would be used for the calculation at the load increase, the overestimation of the overshoots of 6.1 K (for 6333/9686 W) and 6.6 K (for 4441/10636 W) would be made. The exposed results lead to the conclusion that the procedure from [5] cannot deliver transient hot-spot temperature with high precision.

As explained in Section III, the original thermal model of the authors is not suitable to describe the overshoot of hot-spot minus top pocket oil temperature difference. That is why the results of other top oil temperatures values were investigated. In Figs. 4 and 5, the results of using oil at the channel top and oil 3 mm from the winding surface at its top are shown. The records are given for the same test as for Fig. 3.

For the top oil 3 mm from the outer winding surface, the overshoot of the temperature difference amounts to 27%—Fig. 5, which is less than for the top pocket oil (35%—Fig. 3), but still substantial. For oil at the channel top, the overshoot does not exist at all. Unfortunately, the measurement of this temperature is connected with huge practical problems and the calculation procedures should not be based on this temperature. Due to the quoted facts and since the top oil temperature is strongly variable from point to point, the idea of using the bottom oil was proven. The hot-spot to bottom oil temperature difference

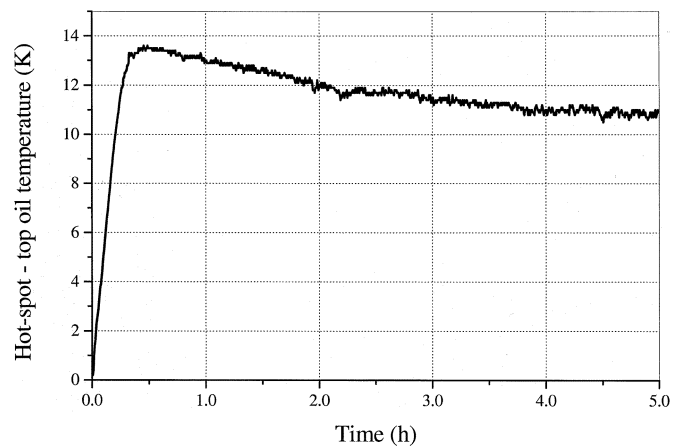


Fig. 5. Hot-spot minus top oil 3 mm from the winding temperature.

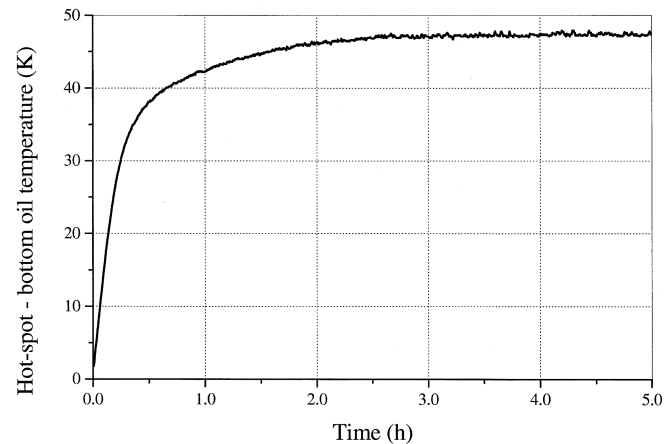


Fig. 6. Hot-spot minus bottom oil temperature.

is shown in Fig. 6. The shape is “promising” since it contains no overshoot. The additional three transients are shown in Fig. 7 in order to confirm a general validity of the conclusion. Since the overshoot does not exist, the bottom oil temperature is convenient to be used as characteristic oil temperature in the original thermal model.

2) *Hot-Spot Temperature Based on Easy Measurements:* Due to the exposed results, (6) is used to calculate the hot-spot

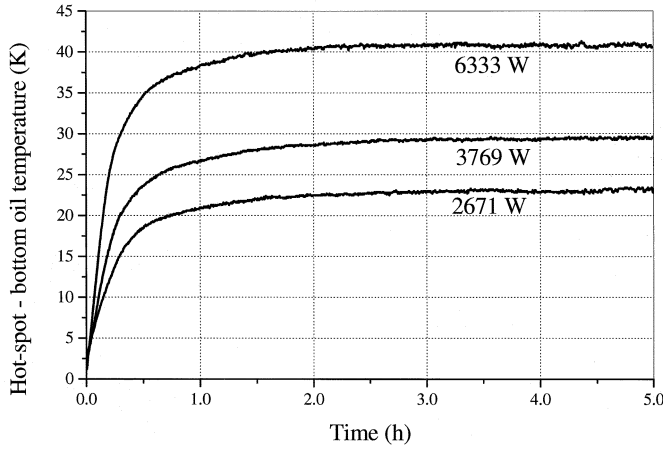


Fig. 7. Hot-spot minus bottom oil temperature at constant loads.

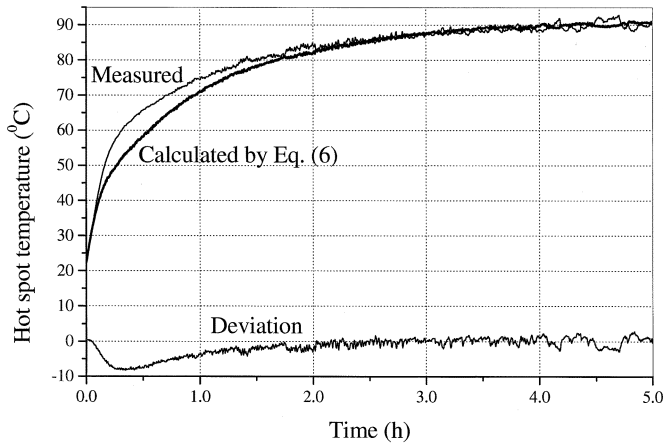


Fig. 8. Error in hot-spot temperature calculation by (6).

temperature. The difference of the hot-spot temperature calculated by (6) and the one obtained by direct measurements (the same test as for Fig. 3) is shown in Fig. 8. In this transient thermal process, the maximal deviation amounts to  $-8.20$  K. In other short-circuit tests with increasing or decreasing loads, high deviations also appeared (maximal absolute deviations in the range  $3.7$ – $8.2$  K).

It will be shown that the error is caused by the time delay of the calculated oil at the top of the winding to bottom oil temperature difference. Equation (6) can be written in the form

$$\theta_{hs}^* = \theta_{bo} + \left(1 - \frac{H}{2}\right)(\theta_{rt} - \theta_{rb}) + H(\theta_{Cua} - \theta_{bo}) \quad (9)$$

where the supposed error is extracted in the term  $(1 - H/2)(\theta_{rt} - \theta_{rb})$ . In Fig. 9, this value is compared with the corresponding one calculated using measured temperature at the top of cooling channel ( $\theta_{toc}$ ):  $(1 - H/2)(\theta_{toc} - \theta_{bo})$ .

The result shows the error in oil at windings top temperature calculation is of similar shape as the error in hot-spot temperature calculation using (6).

To eliminate the quoted error, the following idea for hot-spot temperature definition during one-step load increase or decrease has appeared.

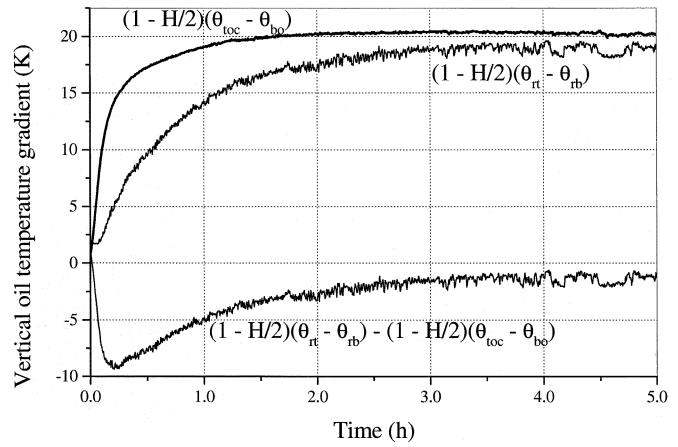


Fig. 9. Error in the calculation of the oil vertical temperature difference.

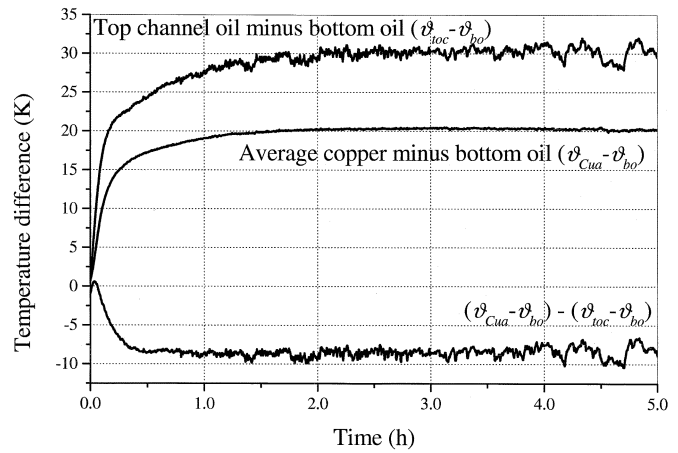


Fig. 10. Components of the top to bottom oil temperature difference.

- 1) The steady-state top minus bottom radiator temperature difference is calculated

$$\Delta\theta_{rt,rbstac} = \theta_{rtstac} - \theta_{rbstac}. \quad (10)$$

- 2) The function  $f(t)$  is defined

$$f(t) = \frac{\theta_{Cua} - \theta_{bo}}{(\theta_{Cua} - \theta_{bo})_{stac}}. \quad (11)$$

- 3) The oil at windings top minus bottom oil temperature difference is equal to

$$\Delta\theta_{to,bo} = \Delta\theta_{rt,rbstac} f(t) \left(1 - e^{-\frac{t}{10 \text{ min}}}\right). \quad (12)$$

- 4) The hot-spot temperature is equal to

$$\theta_{hs}^{**} = \theta_{bo} + \Delta\theta_{to,bo} + H \left( \theta_{Cua} - \left( \theta_{bo} + \frac{\Delta\theta_{to,bo}}{2} \right) \right). \quad (13)$$

The dynamics of oil at windings top minus bottom oil temperature difference contains the following two components: copper minus bottom oil delay and oil at windings top minus copper delay. The second component can approximately be described by an exponential function with the time constant 10 min. This value is estimated from the measurements at the same test as for Fig. 3, shown in Fig. 10. It can be expected that this time constant does not change significantly from one transformer type to another.

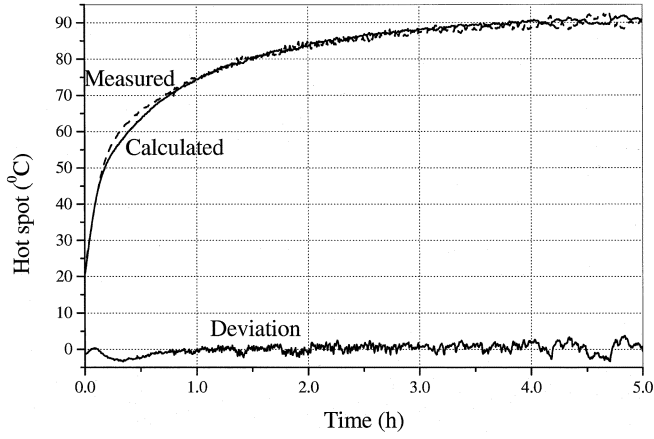


Fig. 11. Result of the proposed hot-spot temperature calculation method.

 TABLE III  
 RANGES OF THE HOT-SPOT CALCULATION ERROR

Experiment	0	0	0	6333	0	0
From/to power (W)	/8667	/3769	/6333	/9686	/2671	/2347
Variable hot-spot factor (see Tab. 1)	$-3.3 \div 3.7$	$-1.8 \div 0.8$	$-2.9 \div 1.7$	$-2.3 \div 2.6$	$-2.6 \div 1.6$	$-2.7 \div 4.8$
Constant hot-spot factor $H = 1.1$	$-1.6 \div 5.5$	$-1.3 \div 1.4$	$-2.7 \div 2$	$-0.3 \div 5.3$	$-1.6 \div 3.5$	$-2.3 \div 3.9$

The result of the method proposed for the same test as for Fig. 3 is shown in Fig. 11. The ranges of the hot-spot temperature calculation error, during different experiments, are exposed in Table III.

## VI. DETERMINATION OF THERMAL MODEL PARAMETERS

As exposed in Section II, parameters of thermal conductances (two parameters for both of the conductances) and two thermal capacitances should be calculated.

After defining the change of the temperatures associated to the nodes of the thermal circuit during the complete transient process of heat experiment, the procedure of the thermal parameters determination [2] can be applied. The temperature associated to the node 2 is simple bottom oil temperature and the temperature associated to the node 1 is calculated from the easily measured temperatures, as described in Section V, using the value of the hot-spot factor  $H = 1.1$ .

Thermal conductances define the steady-states and their parameters can be determined from the measuring results recorded in at least two thermal steady-states. Due to a very sensitive functional form of thermal conductances, it is desirable to have more measurements in order to minimize the error in the calculation of parameters. In the case of using only two steady-states, the measuring error could cause a high error in the exponents ( $n_1$  and  $n_2$ ).

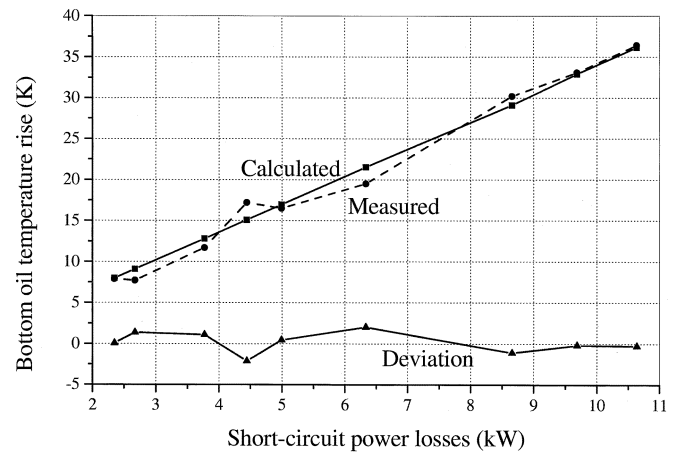
The calculation procedure of power loss distribution is given in [1]. Even in the short-circuit heating experiment, a part of the power loss is located in  $P_2$ . The power  $P_1$  is equal to the copper loss, calculated by the expression

$$P_1 = P_{\gamma Cu} = 3 \cdot 0.65405 \cdot \frac{235 + \vartheta_{Cu}}{255} \cdot I^2 \quad (14)$$

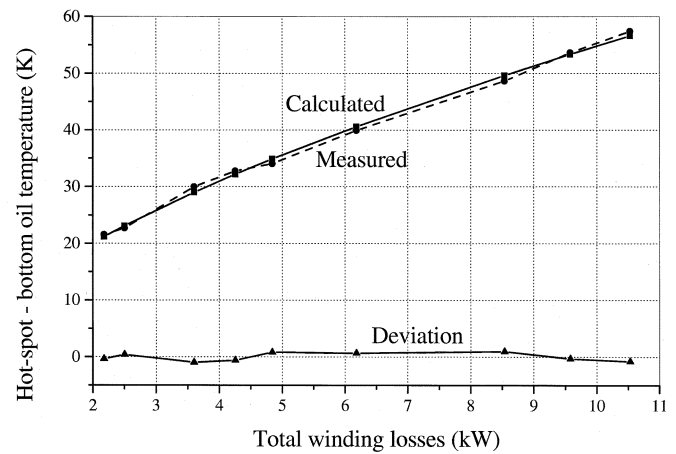
 TABLE IV  
 STEADY-STATE CHARACTERISTIC VALUES

$I$ (A)	$P_{\gamma SC}$ (W)	$P_{\gamma Cu}$ (W)	$P_{\gamma constr}$ (W)	$\vartheta_{hs}$ (°C)	$\theta_{bo}$ (K)	$\vartheta_{hs} - \vartheta_{bo}$ (K)
32	2347	2177	169.6	46.3	7.9	21.6
34.27	2671	2501	170.0	49.9	7.7	22.7
41.18	3769	3600	168.9	54.9	11.7	30.0
43.7	4441	4254	186.9	66.3	17.2	32.8
46.61	4992	4842	150.5	68.9	16.5	34.0
52.54	6333	6181	152.2	70.5	19.5	39.9
60.00	8667	8553	114.0	92.9	30.2	48.7
63.79	9686	9580	106.4	91.7	33.08	53.6
65.6	10636	10530	105.9	104.2	36.4	57.4

$\vartheta_{hs}$  hot-spot temperature, defined by (6);  $H = 1.1$ ;  
 $\theta_{bo}$  temperature rise of the bottom oil;  
 $\vartheta_{hs} - \vartheta_{bo}$  hot-spot minus bottom oil temperature difference.



(a)



(b)

Fig. 12. Steady-state temperature rises.

with  $\vartheta_{Cu}$  average winding temperature,  $I$  the current load, and  $0.65405 \Omega$  the 50-Hz winding resistance at  $20^\circ\text{C}$ .

The power  $P_2$  represents the power loss in construction parts of the transformer due to induced currents ( $P_{\gamma constr.}$ ) and is equal to the difference of total, directly measured value of short-circuit power loss ( $P_{\gamma SC}$ ) and the copper power loss

$$P_2 = P_{\gamma SC} - P_{\gamma Cu} \quad (15)$$

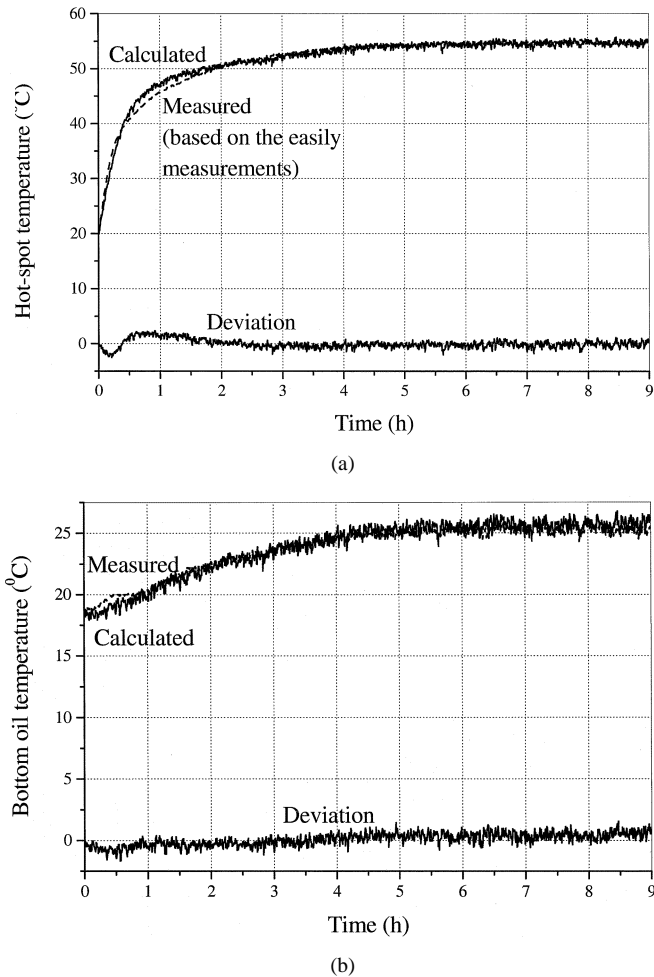


Fig. 13. Experiment used for thermal capacitances estimation.

The results are shown in Table IV.

Based on these results, the parameters of thermal conductances were determined by minimization of the sum of mean square deviation of calculated to measured temperatures. Values of  $\theta_{bo}$  and  $\vartheta_{hs} - \vartheta_{bo}$  obtained by measurement and calculation are shown in Fig. 12. The obtained functional dependencies

$$A_1 = 16.224 (\vartheta_{hs} - \vartheta_{bo})^{0.60454} \text{ and}$$

$$A_2 = 294.302 (\theta_{bo})^0 = 294.30$$

result with maximum deviations of calculated from measured values

$$\Delta\theta_{bo} = 2.11 \text{ K and } \Delta(\vartheta_{hs} - \vartheta_{bo}) = 0.97 \text{ K.}$$

It is interesting to note that although the transformer is with ONAN cooling, thermal conductance  $A_2$  appeared to be constant.

Applying Nelder-Mead simplex (direct search) method [8] to the thermal capacitances estimation, the following values were obtained:  $C_1 = 185.6 \text{ kJ/K}$  and  $C_2 = 2631.2 \text{ kJ/K}$ . For the calculation, the data recorded during the heating experiment with constant power loss, amounting to 3769 W were used. Maximum deviations of calculated from "measured" temperature values in this test were for the hot-spot 2.49 K and for the bottom oil 1.66 K. The calculated and the values predefined based on the easy measurements are shown in Fig. 13.

TABLE V  
MAXIMAL DEVIATIONS OF CALCULATED FROM MEASURED TEMPERATURE VALUES (K)

Experiment From/to power (W)	0 /8667	0 /3769	0 /6333	6333 /9868	0 /2671	0 /2347
Hot-spot temperature, based on the easily measured temperatures	6.03	2.49	5.41	4.50	2.56	3.06
Bottom oil	4.54	1.66	2.70	3.61	1.90	3.33

TABLE VI  
MAXIMAL DEVIATIONS OF CALCULATED FROM DIRECTLY MEASURED TEMPERATURES (K); ONE-STEP LOAD CHANGE

Experiment From/to power (W)	4441 /10636	10636 /5662	0 /8667	0 /3769	0 /6333	6333 /9868	0 /2671	0 /2347
Hot-spot	4.20	6.71	5.07	1.93	3.21	2.69	1.49	3.13
Bottom oil	5.43	4.30	4.53	1.61	2.71	3.65	1.96	3.38

TABLE VII  
MAXIMAL DEVIATIONS OF CALCULATED FROM DIRECTLY MEASURED TEMPERATURES (K); COMPLEX LOAD CHANGE

Experiment	Type	Short-time overload	Short-time overload	Intermittent duty	Intermittent duty	Intermittent duty	Complex daily diagram
	Parameters	$P_b = 4992$ $P_i = 12750$ $t_i = 15$	$P_b = 4992$ $P_i = 12750$ $t_i = 60$	$P_i = 6333$ $t_i = 30$ $P_h = 12750$ $t_h = 30$	$P_i = 6333$ $t_i = 60$ $P_h = 12750$ $t_h = 30$	$P_i = 6333$ $t_i = 15$ $P_h = 12750$ $t_h = 15$	
Hot-spot		6.58	6.62	6.18	6.33	4.87	7.49
Bottom oil		3.91	3.77	3.90	4.33	4.63	7.03

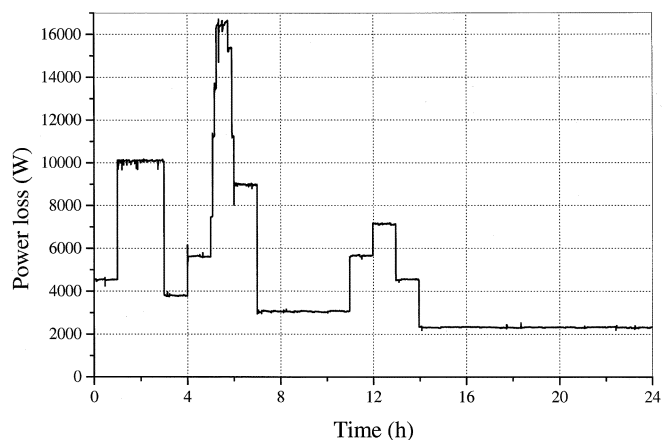


Fig. 14. Complex daily load diagram.

## VII. TEST RESULTS

The results of application of the completely defined thermal model to other tests, in the form of the maximal deviations of calculated from measured temperatures, are shown in Table V.

Since the final goal of the developed procedure is to calculate the real insulation hot-spot temperature, the results delivered by the model are compared with the directly measured hot-spot temperature. The comparison is made for a series of short-circuit heating tests. An overview of the results is exposed in Table VI and Table VII: Table VI contains the results for one-step load

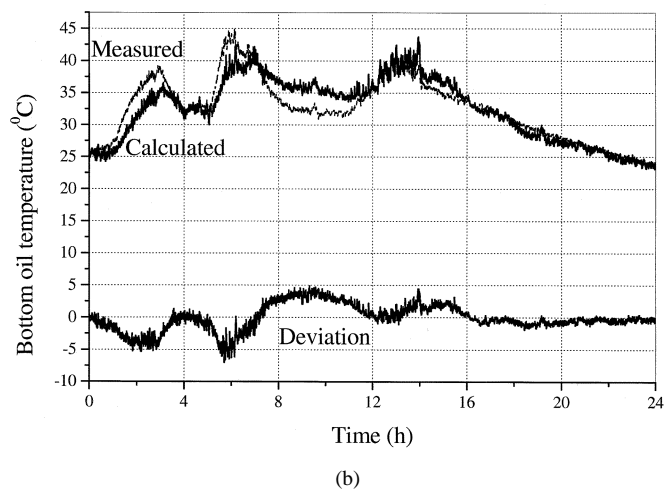
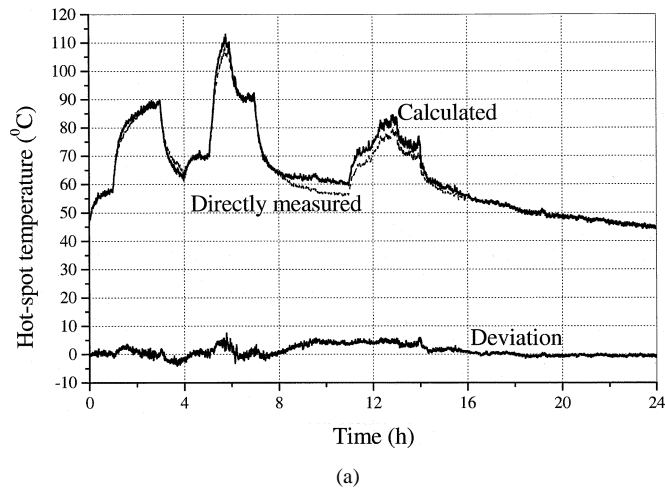


Fig. 15. Results of temperature calculation for the complex daily load diagram (Fig. 14).

change tests and Table VII for more complex test load patterns [2] (short-time overload: basic load  $P_b$ (W) and increased load  $P_i$ (W) of duration  $t_i$ (min), intermittent duty: lower load  $P_l$ (W) of duration  $t_l$ (min) and higher load  $P_h$ (W) of duration  $t_h$ (min); real complex daily diagram, shown in Fig. 14).

Fig. 15 shows calculated and directly measured temperatures of the hot-spot and the bottom-oil for the complex daily load diagram test from Fig. 14. In Fig. 16, different calculation algorithms are compared: the originally developed one, the one from valid IEC standard, and the one from draft of the new standard. Maximal calculation errors are: for the one from valid standard 14.75 K and for the one from draft: 18.26 K. It should be noted that the algorithm from the new IEC draft delivers high calculation errors in the range of the highest load, what especially discredits this algorithm.

### VIII. CONCLUSIONS

The complete procedure for the hot-spot temperature calculation of ONAN transformers is exposed in the paper. The first

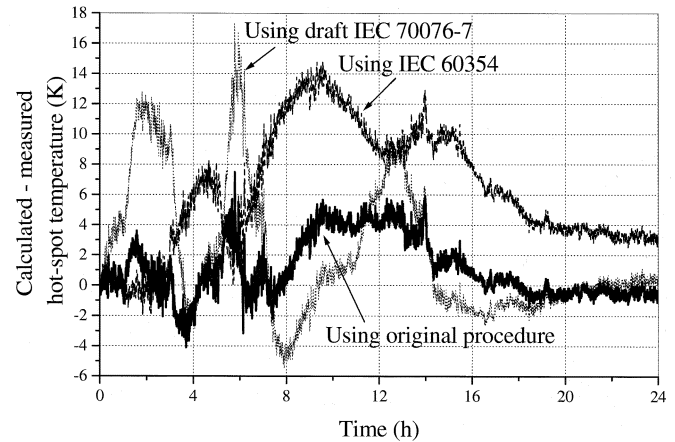


Fig. 16. Comparison of different calculation methods.

step is to define the hot-spot temperature change during the short-circuit heating experiment with constant power loss based on easily measured temperatures: the local ones outside a transformer tank and the average winding temperature. The second step is to determine the parameters of the thermal equivalent circuit with two nodes. After this step, the thermal model is fully defined. The third step is to calculate the hot-spot temperature in conditions of real operation. The input quantities are power losses, precisely calculated and distributed between nodes, and ambient air temperature. The calculation of temperatures corresponding to the nodes of the thermal circuit performs through the numerical solution of the system of two nonlinear differential equations. The test of the complete procedure proposed is done on a 630-kVA ONAN transformer. The maximal error of the hot-spot temperature calculation in the series of tests appeared to be 7.5 K.

### REFERENCES

- [1] Z. Radakovic, "Numerical determination of characteristic temperatures in directly loaded power oil transformer," *Eur. Trans. Elect. Power*, vol. 13, pp. 47–54, Jan./Feb. 2003.
- [2] Z. Radakovic and D. Kalic, "Results of a novel algorithm for the calculation of the characteristic temperatures in power oil transformers," *Elect. Eng.*, vol. 80, pp. 205–214, June 1997.
- [3] L. W. Pierce, "An investigation of the thermal performance of an oil filled transformer winding," *IEEE Trans. Power Delivery*, vol. 7, pp. 1347–1358, July 1992.
- [4] J. Aubin and Y. Langhame, "Effect of oil viscosity on transformer loading capability at low ambient temperatures," *IEEE Trans. Power Delivery*, vol. 7, pp. 516–524, Apr. 1992.
- [5] *IEC Loading Guide for Oil-Immersed Power Transformers*, IEC Std. 60076-7—Power transformers—Part 7, Committee draft 14/403/CD, Oct. 2001.
- [6] *IEC Loading Guide for Oil Immersed Transformers*, IEC Std. 60 354, Sept. 1991.
- [7] Z. Radakovic and Z. Lazarevic, "Novel methods for determining characteristic quantities for developing a thermal model of power transformers," in *Proc. 31st Universities Power Eng. Conf.*, 1996, pp. 481–485.
- [8] MATLAB Version 6.1.0.450 (R12.1) on PCWIN.



**Zoran Radakovic** was born in Belgrade, Yugoslavia, on May 27, 1965. He received the B.Sc., M.Sc., and Ph.D. degrees from the Department of Electrical Engineering at the University of Belgrade, in 1989, 1992, and 1997, respectively.

Currently, he is Associate Professor at the University of Belgrade and is a Humboldt Research Fellow. His research interests include power oil transformer loading, temperature control, harmonic distortion in distribution systems, and the use of bentonite in grounding systems. He is the author of a book on electroheat and many scientific papers.

**Kurt Feser** (F'89) was born in Garmisch Partenkirchen, Germany, on December 10, 1938. He graduated in 1963 and received the Ph.D. degree from the Technical University of Munich, Germany, in 1970.

Currently, he is the Head of the Power Transmission and High Voltage Institute at the University of Stuttgart, Germany. His research interests include asset management in power systems, power transformer monitoring, and diagnosis and electromagnetic compatibility. He is the author of many papers and four patents.

Dr. Feser received honorary degree from University of Breslau, Poland. He also received the Baker Prize Award in 1983. He is chairman of IEC TC 42 (high voltage test technique).